Biotechnology Reports 6 (2015) 108–111

Contents lists available at ScienceDirect

Biotechnology Reports

journal homepage: www.elsevier.com/locate/btre

Short communication

Protein freeze concentration and micro-segregation analysed in a temperature-controlled freeze container

Ulrich Roessl [a,b], Stefan Leitgeb [a], Bernd Nidetzky [a,b,*]

[a] Research Center Pharmaceutical Engineering GmbH, Inffeldgasse 13, A-8010 Graz, Austria
[b] Institute of Biotechnology and Biochemical Engineering, Graz University of Technology, Petersgasse 12, A-8010 Graz, Austria

ARTICLE INFO

Article history:
Received 17 February 2015
Received in revised form 24 March 2015
Accepted 24 March 2015
Available online 26 March 2015

Keywords:
Confocal laser scanning microscopy
Freeze and thaw processing
Freeze concentration
Protein preservation and storage
Stability
Visualization

ABSTRACT

To examine effects of varied freezing conditions on the development of spatial heterogeneity in the frozen protein solution, macroscopic freeze concentration and micro-segregation of bovine serum albumin (BSA) were investigated in a temperature-controlled 200-ml freeze container. Freezing to −40 °C promoted formation of protein concentration gradients (69–114 μg ml^{-1}) in frozen samples taken from 12 different freezer positions, whereby slow freezing in 4 h or longer facilitated the evolution of strong spatial heterogeneities and caused local concentration increases by 1.15-fold relative to the initial protein concentration (100 μg ml^{-1}). To visualize protein micro-segregation during phase separation, BSA was conjugated with fluorescein isothiocyanate and confocal laser scanning fluorescence microscopy was used to localize and size the freeze-concentrated protein regions. Slow freezing resulted in distinctly fewer and larger protein domains in the frozen bulk than fast freezing. Surface stress on the protein during freezing would therefore be minimized at low cooling rates; microscopic freeze concentration would however be highest under these conditions, potentially favoring protein aggregation.

1. Introduction

Proteins are high-value products of biotechnology with a rapidly growing importance on pharmaceutical markets [4,19,27]. The high costs of their production (e.g. Ref. [16]) makes it necessary that proteins are stabilized and stored with only minimum alteration of their biological activity [2,21,26]. Besides freeze drying [6,7,15], freezing is often used for preservation and storage of protein solutions [9,22]. Physically, freezing involves partitioning of the protein solution into an ice phase and a freeze-concentrated liquid [1]. Proteins like other solutes are rejected from the ice [8]. Spatial segregation of the protein is thus induced [5,25]. The consequent change in microenvironment involves various stresses on the protein, including exposure to solid ice surfaces and molecular crowding, which can result in unfolding and aggregation [5,13,20,24,28]. The freezing process should be designed to minimize loss of product quality due to critical stresses incurred. Understanding of how process control variables (e.g. the cooling rate, degree of supercooling) impact the freezing-induced phase separation at different scales would be highly important to assess consequent effects on protein stability [3,9–11,12,14,22]. Studies at microliter scale have quantified spatial heterogeneity in frozen lysozyme solutions prepared by different freezing protocols, showing a protein freeze concentration by up to 7-fold [5]. Denaturation of lysozyme at the interface region of ice and liquid was also demonstrated [5]. However, in view of freezing as a unit operation of industrial biotechnology, investigations of the freezing-induced phase separation and the resulting protein freeze concentration must also be performed at larger scale and in controlled apparatus of defined geometry [9,10,17,22]. Here, evidence from freezing solutions of bovine serum albumin in a temperature-controlled 200 ml freeze container [18] is presented.

2. Materials and methods

2.1. Materials

BSA was from Sigma–Aldrich. Fluorescein isothiocyanate (FITC) and other chemicals were from Roth.

2.2. FITC labeling

2.3 ml of FITC solution (1 mg ml^{-1}) in anhydrous DMSO was added in 20-μl aliquots under gentle stirring to 20 ml of BSA solution (5 mg ml^{-1}, 0.5 M sodium carbonate buffer, pH 9.5). After

* Corresponding author at: Institute of Biotechnology and Biochemical Engineering, Graz University of Technology, Petersgasse 12, A-8010 Graz, Austria.
Tel.: +43 316 873 8400; fax: +43 316 873 8434.
E-mail address: bernd.nidetzky@tugraz.at (B. Nidetzky).

http://dx.doi.org/10.1016/j.btre.2015.03.004

incubation for 12 h at 4 °C in the dark, 2.2 ml of 0.5 M NH_4Cl solution was added and incubation continued for 2 h. Unbound FITC was removed and buffer exchanged to 50 mM potassium phosphate (pH 7.5) using Vivaspin ultrafiltration. The molar FITC/BSA ratio (F/P) was determined with the relationships:

$$\frac{F}{P} = \frac{A_{495}}{A_{280} - (0.35 \times A_{495})/0.614} \times C$$

$$C = 0.876 = \frac{66{,}433}{389 \times 195}$$

66,433 and 389 are BSA and FITC molecular weight, respectively; 195 is absorption $E^{0.1\%}$ of bound FITC at 490 nm, $(0.35 \times A_{495})$ is a correction factor for FITC absorbance at 280 nm [11], and 0.614 is BSA absorption at 280 nm at 1.0 mg ml^{-1}. Absorbances measured (A) are given with wavelength in subscript. They were recorded on a Beckman Coulter DU 800 spectrophotometer.

2.3. Freezing, sampling, sample processing and analysis

Native BSA and FITC-labeled BSA were used. About 200 ml of protein solution (0.1 mg ml^{-1}) were frozen in a freeze container (described in Ref. [18]) Silicone oil (M40.165.10 by Huber, Germany) was used as thermofluid. The different freezing protocols applied are described in Section 3. Temperature inside the freeze container was measured with 8-channel PCE-T 800 Multi-Input Thermometer, with probes at seven positions (A–G) indicated in Fig. 1. Freezing time was defined as the time between nucleation and complete solidification of the bulk, which can be identified as a plateau in the measured temperature profiles [18]. When seeding was performed, frozen buffer droplets were introduced next to the cooled container walls as soon as the bulk temperature was −2 °C.

After freezing and equilibration of bulk temperatures, the ice block was removed from the container. For native BSA concentration determination, the removed ice block was cut into pieces (1–12) as indicated in Fig. 1. The samples were thawed, and the soluble BSA concentration was measured in each of them. Roti-Nanoquant protein assay was used. The FITC label interfered with protein determination, thus precluding the same protein analysis when using the FITC–BSA conjugate.

To perform confocal laser scanning microscopic analysis on frozen material, samples were drilled from the frozen ice block using a hollow drill with an inner diameter of 25 mm. From each run three samples were taken from positions I–III, as shown in Fig. 1. Ice cores were stored in 50-ml Falcon tubes at −70 °C until microscopic examination. Images were obtained with a Leica DMI 6000 inverted microscope in a TCS SP5 system. Excitation was at 488 nm, acquisition from 502 to 603 nm. It should be noted that images presented later on were chosen to represent the predominant microscopic appearance of the probed position. However, between 5 and 8 CLSM images with adequate quality were taken from each position. In addition, for every sample at least one acquisition of stacked images in z-direction was performed, each stack containing approx. 50–100 single images. Every single or stacked image pictured an area of 620 × 620 μm. It was ensured through careful comparison of different sample areas that the images shown are fully representative for the frozen sample as a whole. Images were collected as fast as possible before any sample melting through laser beam exposure could occur.

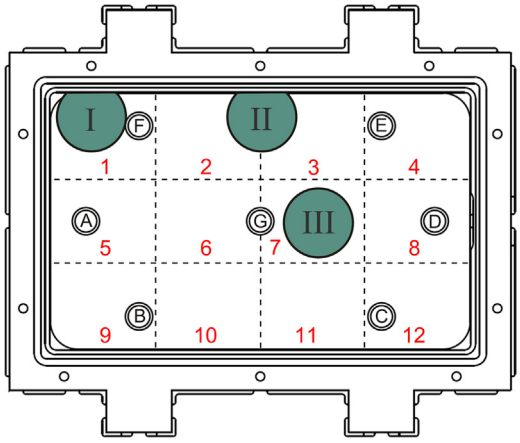

Fig. 1. Schematic illustration of the freeze container with sampling positions 1–12 and I–III indicated. Thermocouples at positions (A–G) are also shown.

3. Results

3.1. Macroscopic freeze concentration of BSA

Using a common thermofluid set temperature of −40 °C, solutions of unlabeled BSA were frozen at different freezing rates. The fastest freezing rate involved immediate switch from room to set temperature. Relatively slower freezing rates involved linear temperature ramps from room to set temperature over 4 h and 14 h. Freezing over the 4 h temperature ramp involved an additional seeding step. No seeding was applied during the 14 h temperature ramp in order to maximize the effect of supercooling. The rapid lowering of temperature during fast freezing resulted in immediate nucleation at the container walls, thus making seeding unnecessary. Aim of the experiments was to evaluate the influence of the freezing protocol on freeze concentration at 12 different points in the freeze container (see Fig. 1). Results are summarized in Table 1. Analysis of the protein distribution across the different sampling positions 1–12 is based on a total protein recovery of 95% or greater.

Spatial characteristics of BSA freeze concentration were similar in each experiment where protein concentrations were highest in the slowly freezing central region of the container around the longitudinal axis, in particular at positions 6 and 7. In container side regions that froze fastest (positions 1, 4, 9 and 12), by contrast, BSA concentrations were lowest. The freeze concentration can be characterized by the maximum and minimum protein concentrations observed across the container. Slowing down the freezing rate resulted in increased protein concentrations in the maximally freeze-concentrated regions of the container. The minimum protein concentration was lowest for the seeded 4-h freezing run, and also the ratio between maximum and minimum protein concentration was highest under these conditions. Maximum/minimum protein concentration ratios of between 1.4 and 1.7 indicate macroscopic freeze concentration to have been substantial under all freeze conditions used.

Considering the protein distribution in frozen bulk (Table 1) and assuming comparable cryoconcentration patterns of labeled and unlabeled BSA, positions I–III were chosen in regions with low, intermediate and high protein concentrations to obtain samples for microscopic imaging by CLSM analysis.

3.2. Visualization of the distribution of freeze-concentrated FITC–BSA conjugate

The FITC-labeled BSA preparation used had a F/P ratio of 3.4. For CLSM imaging experiments, fast freezing (freezing time = 53 min) and 4-h seeded freezing (freezing time = 87 min) were performed as in Table 1. In addition, a 4-h freezing run was done without seeding (freezing time = 73 min) to induce supercooling. Seeding

Table 1
Spatially resolved protein distribution in BSA solutions frozen at different freezing rates (fast, 4 h, 14 h) to thermofluid temperature of −40 °C. Sampling positions 1–12 refer to Fig. 1. *N* is the number of replicate freezing runs. Seeding was performed in the 4-h freezing run. Results are given in percent concentration (*C*) where 100% equals the initial solution concentration of 0.1 mg l^{-1}. Mean values ± standard deviations are shown. Range = $C_{max} - C_{min}$; Ratio = C_{max}/C_{min}.

Freeze rate	1	2	3	4	5	6	7	8	9	10	11	12	Range	Ratio
Fast *N* = 5	86 ± 5	91 ± 8	92 ± 5	86 ± 7	100 ± 13	102 ± 10	104 ± 8	95 ± 9	77 ± 6	84 ± 4	86 ± 7	80 ± 3	31 ± 9	1.4 ± 0.1
4 h *N* = 3	70 ± 7	82 ± 6	83 ± 6	78 ± 3	88 ± 6	110 ± 6	109 ± 4	93 ± 5	69 ± 2	77 ± 6	78 ± 8	72 ± 4	45 ± 4	1.7 ± 0.1
14 h *N* = 3	80 ± 2	87 ± 3	91 ± 2	85 ± 2	104 ± 5	113 ± 2	114 ± 5	110 ± 2	75 ± 5	78 ± 6	81 ± 5	78 ± 4	40 ± 1	1.5 ± 0.04

was however used in the slow-freezing run where set temperature was decreased linearly to −40 °C within 12 h (freezing time = 4 h 22 min). Note that the set temperature decreases were comparable but not identical to the freezing experiments described in Table 1.

Representative images from CLSM analysis of ice core samples are shown in Fig. 2 where images are arranged by position and freezing time. Note: in the non-seeded 4-h freezing experiment (freezing time = 73 min), supercooling was achieved in the whole bulk whereby just before spontaneous nucleation, temperatures of −4.6 °C and −1.0 °C were recorded in peripheral (thermocouples B, C, F, E in Fig. 1) and central regions of the freeze container (thermocouples A, G, D in Fig. 1), respectively.

In most of the sample images, irregular distributions of labeled protein were found. Protein was accumulated in localized and contained regions, circular or elongated in shape and approximately 10–100 μm in diameter or length. Ice growth direction could be identified from the parallel alignment of the concentrated protein regions at freezing times of 87 min and 4 h 22 min (position I + II) as well as after 53 min (position I). In the central position III, protein inclusions appeared unordered, irrespective of the freezing time.

The distance between the freeze-concentrated regions varied with the duration of freezing. In positions I–II, distances increased from a few 10 μm at short freezing time to several 100 μm at high freezing time. The size of protein domains was biggest at the slowest freezing time (4 h 22 min), in any of the three sampling positions.

4. Discussion

Freezing induced a substantial amount of macroscopic spatial heterogeneity in BSA solutions (Table 1). Maximum BSA concentration in freeze-concentrated regions increased on increase in the freezing time. Ratio between maximum and minimum protein concentration also changed on variation of the freezing rate. Explanations for the macroscopic observations were found through analysis of microscopic effects of the freezing, as follows.

Of the sampling positions selected for CLSM analysis, position III was located in the freeze container's very last point to freeze and as expected, it was the one to show the highest protein concentration. The remaining positions (I, II) represented faster freezing points of the container, and they exhibited decreased protein concentration. Fig. 2 shows that freeze-concentrated protein regions were formed in larger number and bigger size at sampling position III, as compared to positions I and II, under conditions of slow freezing (87 min, 4 h 22 min). The effect was weakened (73 min) or even absent (53 min) at faster freezing rates.

Fig. 2 also shows that slower freezing times (87 min, 4 h 22 min) resulted in fewer and larger freeze-concentrated regions and also in wider protein-free regions, except for position III (see below).

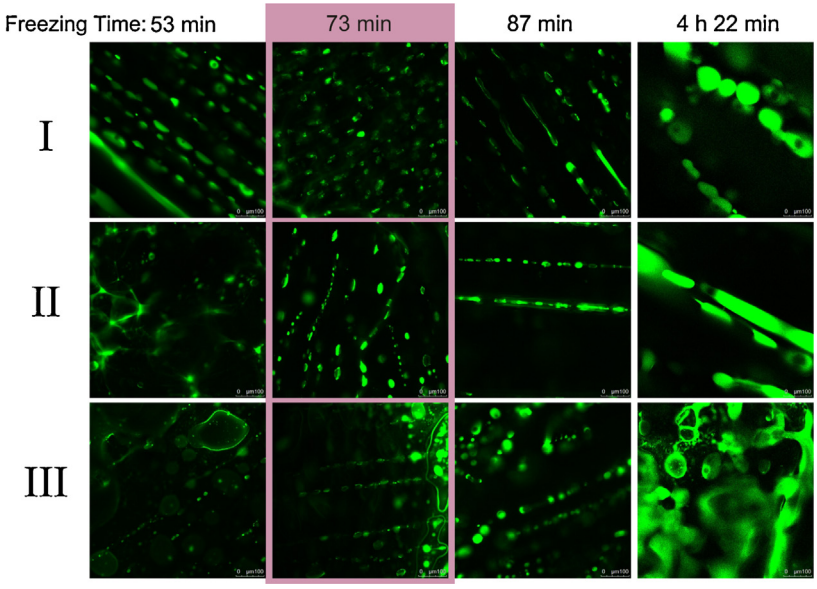

Fig. 2. CLSM images from frozen FITC–BSA core samples taken at positions I–III. The applied freezing times are indicated. Note: freezing time measures the time between nucleation and complete solidification of the bulk. It is not the full time of the freezing experiment. In the highlighted experiment (pink), no seeding was performed. Images were obtained with a Leica DMI 6000 inverted microscope in a TCS SP5 system. Excitation was at 488 nm, acquisition from 502 to 603 nm. Magnification was 630-fold. Samples were placed in a plastic dish with a glass slide bottom while dry ice was used for cooling. Images were collected as fast as possible before any sample melting through laser beam exposure could occur. Multiple images were collected from each position. It was ensured through careful comparison of different sample areas that the images shown were fully representative for the frozen sample as a whole. (For interpretation of the references to color in this figure legend, the reader is referred to the web version of this article.)

Faster freezing, by contrast, caused a higher number of smaller freeze-concentrated regions, as revealed on comparing the 53 min and 4 h 22 min freezing runs at the position I and position II. The effect of seeding is made evident by comparing the 73 min and 87 min freezing runs. In the non-seeded 73 min run, freeze-concentrated protein regions were much smaller and distributed in a way more irregular fashion than in the seeded 87 min run. Microscopic protein distribution at position I is relevant in particular: almost instant solidification of the whole sampling position was noticed after spontaneous nucleation whereas in the seeded experiment, the freezing occurred much slower in this region. The comparably regular (linear) appearance of freeze-concentrated protein regions in the seeded experiment is therefore noted, at position I but also at position II. Linear alignment of the protein domains could be caused by dendritic ice growth, which is often found in bulk-scale freezing [23]. One expects dendritic growth to be pronounced under conditions where solidification occurs relatively slow, as in the seeded experiment with its low degree of supercooling.

There are practical ramifications of the evidence presented. Formation of a relatively large number of freeze-concentrated protein domains under conditions of fast freezing implies pronounced exposure of proteins to ice crystal surfaces. High cooling rates could therefore be unfavorable for freezing of surface-sensitive proteins. At slow freezing rates, fewer and larger protein domains are present. It is quite likely that the protein concentration will be higher in the large as compared to the small domains and therefore, slow freezing may create problems with proteins having low solubility limits and tend to native-like aggregation.

Acknowledgements

Heimo Wolinski (Institute of Molecular Biosciences, University of Graz) assisted the CLSM analysis. Support from Zeta Biopharma is acknowledged. This work was funded within the Austrian COMET Program under the auspices of the Austrian Federal Ministry of Transport,Innovation and Technology (bmvit), the Austrian Federal Ministry of Economy, Family and Youth (bmwfj), and the State of Styria (Styrian Funding Agency SFG). The COMET Program is managed by the Austrian Research Promotion Agency (FFG).

References

[1] A. Bogdan, M.J. Molina, H. Tenhu, et al., Visualization of freezing process in situ upon cooling and warming of aqueous solutions, Sci. Rep. 4 (2014) 7414.
[2] J.W. Bye, L. Platts, R.J. Falconer, Biopharmaceutical liquid formulation: a review of the science of protein stability and solubility in aqueous environments, Biotechnol. Lett. 36 (2014) 869–875.
[3] E. Cao, Y. Chen, Z. Cui, et al., Effect of freezing and thawing rates on denaturation of proteins in aqueous solutions, Biotechnol. Bioeng. 82 (2003) 684–690.
[4] T. Dingermann, Recombinant therapeutic proteins: production platforms, challenges, Biotechnol. J. 3 (2008) 90–97.
[5] J. Dong, A. Hubel, J.C. Bischof, et al., Freezing-induced phase separation and spatial microheterogeneity in protein solutions, J. Phys. Chem. B 113 (2009) 10081–10087.
[6] M.I. Esteves, W. Quintilio, R.A. Sato, et al., Stabilisation of immunoconjuagtes by trehalose, Biotechnol. Lett. 22 (2000) 417–420.
[7] Y. Grant, P. Matejtschuk, C. Bird, et al., Freeze drying formulation using microscale and design of experiment approaches: a case study using granulocyte colony-stimulating factor, Biotechnol. Lett. 34 (2012) 641–648.
[8] K. Izutsu, S. Kojima, Freeze-concentration separates proteins and polymer excipients into different amorphous phases, Pharm. Res. 17 (2000) 1316–1322.
[9] P. Kolhe, E. Holding, A. Lary, et al., Large-scale freezing of biologics: understanding protein and solute concentration changes in a cryovessel – part 2, BioPharm Int. 23 (2010) 40–49.
[10] P. Kolhe, E. Amend, S.K. Singh, Impact of freezing on pH of buffered solutions and consequences for monoclonal antibody aggregation, Biotechnol. Progr. 26 (2010) 727–733.
[11] P. Kolhe, A. Badkar, Protein and solute distribution in drug substance containers during frozen storage and post-thawing: a tool to understand and define freezing–thawing parameters in biotechnology process development, Biotechnol. Progr. 27 (2011) 494–504.
[12] L.A. Kueltzo, W. Wang, T.W. Randolph, et al., Effects of solution conditons, processing parameters, and container materials on aggregation of a monoclonal antibody during freeze-thawing, J. Pharm. Sci. 97 (2008) 1801–1812.
[13] L. Liu, L.J. Braun, W. Wang, et al., Freezing-induced perturbation of tertiary structure of a monoclonal antibody, J. Pharm. Sci. 103 (2014) 1979–1986.
[14] M.A. Miller, M.A. Rodrigues, M.A. Glass, et al., Frozen-state storage stability of a monoclonal antibody: aggregation is impacted by freezing rate and solute distribution, J. Pharm. Sci. 102 (2013) 1194–1208.
[15] N. Rathore, R.S. Rajan, Current perspectives on stability of protein drug products during formulation, fill and finish operations, Biotechnol. Progr. 24 (2008) 504–514.
[16] D. Reinhart, R. Kunert, Upstream and downstream processing of recombinant IgA, Biotechnol. Lett. 37 (2015) 241–251.
[17] M.A. Rodrigues, M.A. Miller, M.A. Glass, et al., Effect of freezing rate and dendritic ice formation on concentration profiles of proteins frozen in cylindrical vessels, J. Pharm. Sci. 100 (2010) 1316–1329.
[18] U. Roessl, D. Jajcevic, S. Leitgeb, et al., Characterization of a laboratory-scale container for freezing protein solutions with detailed evaluation of a freezing process simulation, J. Pharm. Sci. 103 (2013) 417–426.
[19] M. Sabalza, P. Christou, T. Capell, Recombinant plant-derived pharmaceutical proteins: current technical and economic bottlenecks, Biotechnol. Lett. 36 (2014) 2367–2379.
[20] J.J. Schwegman, J.F. Carpenter, S.L. Nail, Evidence of partial unfolding of proteins at the ice/freeze-concentrate interface by infrared microscopy, J. Pharm. Sci. 98 (2009) 3239–3246.
[21] S.K. Singh, Impact of product-related factors on immunogenicity of biotherapeutics, J. Pharm. Sci. 100 (2012) 354–387.
[22] S.K. Singh, P. Kolhe, W. Wang, et al., Large-scale freezing of biologics; a practitioner's review. Part one: fundamental aspects, Bioprocess Int. 7 (2009) 32–44.
[23] S.K. Singh, S. Nema, Freezing and thawing of protein solutions, in: F. Jameel, S. Hershenson (Eds.), Formulation and Process Development Strategies for Manufacturing Biopharmaceuticals, JohnWiley & Sons, Hoboken, 2010, pp. 625–675.
[24] G.B. Strambini, M. Gonnelli, Protein stability in ice, Biophys. J. 92 (2007) 2131–2138.
[25] A. Twomey, R. Less, K. Kurata, et al., In situ spectroscopic quantification of protein–ice interactions, J. Phys. Chem. B 117 (2013) 7889–7897.
[26] M.M.C. Van Beers, M. Bardor, Minimizing immunogenicity of biopharmaceuticals by controlling critical quality attributes of proteins, Biotechnol. J. 7 (2012) 1473–1484.
[27] G. Walsh, Biopharmaceutical benchmarks 2014, Nat. Biotechnol. 32 (2014) 992–1000.
[28] A. Zhang, S.K. Singh, M.R. Shirts, et al., Distinct aggregation mechanisms of monoclonal antibody under thermal and freeze–thaw stresses revealed by hydrogen exchange, Pharm. Res. 29 (2012) 236–250.